

# Impact of Rainfall on 5G Millimeter Wave Channels

Lee Loo Chuan<sup>1</sup>, Mardeni Roslee<sup>1,\*</sup>, Chilakala Sudhamani<sup>1</sup>, Sufian M. I. Mitani<sup>2</sup>,  
A. Waseem<sup>3</sup>, Anwar F. Osman<sup>4</sup>, Fatimah Z. Ali<sup>5</sup>, and Yasir Ullah<sup>1</sup>

<sup>1</sup>Faculty of Engineering, Multimedia University, Cyberjaya 63100, Selangor, Malaysia

<sup>2</sup>Telekom Malaysia Research & Development, Malaysia

<sup>3</sup>Department of Electrical Engineering, International Islamic University, Islamabad 44000, Pakistan

<sup>4</sup>Spectre Solution Sdn Bhd, Malaysia

<sup>5</sup>Faculty of Electrical Engineering, Universiti Teknologi MARA, Shah Alam 40450, Selangor, Malaysia

**ABSTRACT:** Wireless connections in 5G technology are driving the rapid growth of intelligent transport systems and vehicle communications. Wireless channels are impacted by weather, which is most noticeable in millimeter wave bands. This includes rain, fog, snow, sand, and dust. 5G networks now support diverse applications with speed and quality. In an effort to enable the use of millimeter wave frequencies, a recent study examined the impact of dust and sand on 5G channels. This paper examines the impact of heavy and frequent rainfall, along with horizontal polarization, on the propagation of millimeter waves in urban and highway settings. Using theoretical and optimization techniques, the effects of rainfall attenuation, path loss, and connection margin are evaluated at various millimeter wave frequencies. Dependencies on rainfall rate, path variation, and operating frequency are shown by the simulation results. In urban and highway situations, mean path loss and error statistics are examined with and without rainy attenuation. It is observed that the particle swarm optimization approach achieves 94% accuracy in signal propagation, which will enhance the path loss, received power, and overall system performance.

## 1. INTRODUCTION

The increasing demand for higher data rates, wider coverage, and enhanced capacity has motivated the research and development of 5G communication network. 5G and beyond uses un-utilized millimeter wave (mmwave) frequencies above 10 GHz [1], as there is scarcity for spectrum below 5 GHz. These higher frequencies enhance the throughput, spectral efficiency, and network efficiency [2, 3]. However, high-frequency mmwave signal travels only shorter distances due to its atmospheric absorption. Furthermore, the signal quality is influenced by propagation paths, such as line of sight (LOS) or non-line of sight (NLOS), and weather conditions such as rain, fog, snow, dust, and sand. Under all these conditions, the signal energy may experience absorption, scattering, diffraction, or depolarization [4].

In wireless communication networks, LOS propagation is essential to achieving faster data rates and improved quality of service. The signal strength heavily depends on the propagation medium, making LOS propagation especially important in 5G applications, including mmwave and mobile communication [5–7]. However, the signal transmission at mmwave frequencies can be significantly influenced by rainfall rate, which restricts the propagation path length and the use of higher frequencies for LOS communication. Along with the rainfall rate, the size of the raindrop influences the propagating signal by absorbing or scattering the propagating signal energy, which decreases the total received signal power [8]. The signal attenuation also depends on factors such as path length, polarization,

frequency, and latitude. In heavy rainfall regions like Malaysia, the wireless channels often experience interference from frequent and intense rainfall [9]. The attenuation of propagating signals varies with factors such as rain rate, density, drop size, operating frequency, and path length [10, 11]. Rain attenuation forecasting can utilize either physical or empirical models [12], which rely on local environmental conditions and operating frequencies. In [13], the authors estimated the rain attenuation at mmwave frequencies using ITU-R 530-16, Da Silva Mello, and a differential equation model.

The signal reduction increases with the increased rainfall, signal attenuation, and path difference, which will cause path loss (PL) and a reduction in the total coverage area. The term “path loss” refers to the reduction in the wireless signals effective transmitting power as it travels through a channel. This phenomenon is due to variations in the propagation path, presence of obstacles, weather conditions, and antenna characteristics. Antenna directivity, crucial for estimating PL, is determined by factors such as antenna location, tilt angle, and height [14]. PL estimation utilizes various prediction models like LOS and NLOS, indoor and outdoor, long distance and short distance, etc. Various PL models have been extensively discussed in the literature [15–18].

Every state in Malaysia has been evaluated and compared for the impact of rainfall intensity on propagating signals at 26 GHz [15]. Higher PL is correlated with increased attenuation of rainfall. Furthermore, sand and dust particles impair signals’ ability to propagate in some tropical regions. The Mie scattering model [19] is used to estimate the effect of dusty

\* Corresponding author: Mardeni Bin Roslee (mardeni.roslee@mmu.edu.my).

storms on wave propagation. With Mie scattering models, the PL arising from sand and dust is investigated. The wireless channels operating at mmwave frequencies are also affected due to sand and dust [20, 21]. In urban and highway situations, the effect of route loss is calculated for dedicated short-range communication (DSRC) and mmwave frequencies [22]. The effectiveness in terms of bandwidth, throughput, and latency of the 5G test network and its long-term evaluation are compared for various weather and traffic scenarios in real-world settings [23]. A wide range of tactics and technologies intended to improve throughput, optimize data rates, increase capacity, and improve coverage in the context of a 5G network [24].

Precipitation, including rain and fog, modifies the properties of the channel and weakens the signal at various frequencies, like the V-band at 60 GHz and E-band at 73 GHz. The authors also investigate how temperature and humidity, especially in the winter, affect wave propagation [25]. In addition, the effects of rainfall and water vapor on E-band transmissions are evaluated [26]. The path loss attenuation rises with increasing rainfall intensity, according to the results. According to a study conducted in Nigeria, mmwave attenuation during periods of intense rainfall is estimated at temporal percentages between 0.01% and 0.001% [27]. In [28], the authors estimated the effect of snow on vehicle-to-vehicle (V2V) communication at 60 GHz and observed that the LOS path distance was shortened to 60 meters compared to normal conditions [28].

Path difference optimization in V2V scenarios is mainly based on free-space path loss and connection margin considerations at two different frequencies: the 5.9 GHz DSRC frequency and 28 GHz 5G frequency [29]. The path differences of 867 m and 688 m are used to demonstrate high data speeds at 27 Mbps and 1 Gbps, respectively. Ground penetrating radar (GPR) mixer model is also used to evaluate the signal loss caused by different road pavement densities at 1.7 GHz to 2.6 GHz [30]. The frequencies of 21.8 GHz (K-band) and 73.5 GHz (E-band) are used in research on rain attenuation [31]. The findings show that when rainfall is less than 108 mm/h, using the E-band frequency improves microwave connection backhaul performance for reaching high data rates and throughput, whereas using the K-band frequency is better when rainfall is more than 108 mm/h. Furthermore, received signal strength is greatly impacted by variables such as user location, mobility, speed of a vehicle, operating frequency, and spectrum hand-off [32–36].

Numerous optimization algorithms were employed to minimize the path loss. In the existing body of literature, several researchers have investigated optimization algorithms for optimizing path differences in both outdoor and indoor environments across diverse frequencies and utilizing various path loss models [37–40]. Path optimization was carried out through the utilization of genetic algorithm (GA), particle swarm optimization (PSO), and ant colony algorithm (ACM). A comparative analysis of the path optimization processes revealed that the performance of ACM outperformed both GA and PSO [37]. Optimal path determination was achieved using PSO and GA methods, leading to the observation that PSO generated optimal path loss outcomes more rapidly than GA [38]. The preci-

sion of the COST231 model's path loss was enhanced by fine-tuning the model parameters with the application of PSO. The obtained error statistics were compared with various empirical path loss models [39]. Within mixed land-water regions, the empirical COST-Hatta model's path loss was predicted using machine learning algorithms, and the results showcased that the proposed model achieved a remarkable accuracy level of 94.12% [40]. In indoor settings, a polynomial equation-driven PSO technique was employed for the precise estimation of path differences, yielding an 85% reduction in estimated path difference errors [41].

This study investigates the impact of rainfall on the 5G mmwave channel, particularly focusing on PL and link margin evaluation within highway and urban scenarios. We leverage the utilization of PSO and GA optimization algorithms to mitigate path loss and enhance overall system performance. A comparative analysis of error statistics is conducted, revealing that the system's performance is notably elevated through the application of the PSO algorithm, surpassing the theoretical and GA approaches. Moreover, optimal path difference values are derived for both highway and urban settings under varying conditions of rain attenuation. These optimal values contribute to increasing the channel capacity and throughput, thereby facilitating the achievement of higher data rates.

The remainder of the document is structured as follows. Section 2 presents rain attenuation, while Section 3 discusses optimization techniques. Link margin estimations are discussed in Section 4. The simulation results are shown in Section 5. Section 6 contains the conclusions and future scope.

## 2. RAIN ATTENUATION

Rainfall has an impact on wireless channels that operate at frequencies greater than 10 GHz; this effect is especially pronounced in tropical locations where there is a lot of rainfall [42–45]. Two important factors in signal attenuation are rainfall rate and raindrop size. The literature contains a wide range of models for predicting rain attenuation, including statistical, empirical, fade-slope, physical, and optimization models [46–51]. Based on many environmental factors, each model calculates the attenuation of rain. Because statistical models produce realistic results that are especially relevant to tropical places like Malaysia, we chose to use them in this work to forecast rain attenuation. The constant highs and lows, together with regular thunderstorms, characterize Malaysia's tropical climate. The seasonal monsoons — the northeast monsoon, which runs from October to March, and the southeast monsoon, which runs from April to September, are primarily responsible for rainfall rates [52]. By employing the ITU-R P.530-18 model, our goal is to calculate the impact of rain from 1 GHz to 100 GHz with path variations as large as 60 km. According to this model, operating frequency, rain rate, polarization, and path reduction factor all affect how much rain is attenuated [53, 54]. This model does not account for the attenuation caused by hail, fog, or snowfall. Because of this, the ITU-R P.530-18 model is the most reliable model in Malaysia for forecasting rain attenuation.

The PL resulting from precipitation in the outdoor region can be calculated using the ITU-R P.530-18 model as the product of

effective path length ( $D_{eff}$ ) and the attenuation factor ( $\Gamma_A$ ) [54]. Therefore, the total attenuation ( $A$ ) can be written as

$$A = \Gamma_A * D_{eff} \quad (1)$$

The attenuation factor is based on the intensity of the rainfall, which is calculated using the power law relationship from the rain rate ( $\gamma$ ) after a certain amount of time, which is given as

$$\Gamma_A = K \cdot \gamma^\beta \quad (2)$$

where  $\gamma$  is measured in millimeters;  $A$  represents the path attenuation in dB/meter; and  $\Gamma_A$  is an attenuation factor in dB/m. The constants  $K$  and  $\beta$  depend on the signal's polarization and operating frequency ( $f$ ) in GHz, respectively. The lookup table contains the  $K$  and  $\beta$  values for both vertical and horizontal polarizations between 1 GHz and 1000 GHz [55]. The database providing generic weather forecast data is kept up-to-date by the Malaysian Meteorological Department. In order to evaluate path attenuation, we concentrate on the rain rate at 0.01% of the rain.

The path difference ( $D$ ) and the reduction factor caused by the rainfall ( $p_r$ ) after a specific time period are combined to form the effective path length, which is always less than the actual path length. ( $p_r$ ) can be determined by calculating the discrepancy in received signal strength between clear sky conditions and rainy conditions. Therefore, the overall signal attenuation resulting from rainfall is given as

$$A = K \cdot \gamma^\beta \cdot D \cdot p_r \quad (3)$$

( $p_r$ ) is represented as [44]

$$p_r = \frac{1}{0.477R^{0.633}A_{0.01}^{0.073\beta}f^{0.123} - 10.579[1 - \exp(-0.0241D)]} \quad (4)$$

Eq. (4) can be substituted into Eq. (3) to estimate the path loss caused by rainfall.

### 3. LINK MARGIN

In 5G cellular networks, precise PL estimation plays a pivotal role in determining various crucial factors, such as the number of cells required to cover a given region, the total signal loss that occurred due to the propagation path, the transmission power, and the overall system performance. The primary focus of network planning and optimization is to minimize the PL, which is defined as the attenuation or decrease in power that a propagating signal experiences within the propagation path. A wide range of path loss models, each customized to predict path loss depending on certain environmental factors and the kind of transmission media, have been presented in the literature. These models are essential instruments for precisely evaluating signal propagation and maximizing 5G network performance in various deployment scenarios. This paper explores the effect of rainfall on PL in both urban and highway scenarios, as well as in free-space environments. Given the high population density and data demands, we focus on estimating path loss in urban ( $PL^U$ ) and highway ( $PL^H$ ) settings. According to the free space PL model, the cities and highway scenario LOS and

NLOS path losses are estimated as [22]

*LOS Path loss :*

$$PL^U = 38.77 + 16.7 * \log_{10}(D) + 18.2 * \log_{10}(f) \quad (5)$$

$$PL^H = 32.4 + 20 * \log_{10}(D) + 20 * \log_{10}(f) \quad (6)$$

*NLOS Path loss :*

$$PL^{U/H} = 36.85 + 30 * \log_{10}(D) + 18.9 * \log_{10}(f) \quad (7)$$

where  $D$  represents the path difference in meters,  $f$  the operating frequency in GHz, and  $PL$  the path loss in dB. In Malaysia, heavy rainfall will influence the path loss. The modified LOS and NLOS path loss expressions for urban and highway scenarios are given as

*LOS Path loss :*

$$PL_{RF}^U = 16.7 * \log_{10}(D) + 18.2 * \log_{10}(f) + 38.77 + A \quad (8)$$

$$PL_{RF}^H = 20 * \log_{10}(D) + 20 * \log_{10}(f) + 32.4 + A \quad (9)$$

*NLOS Path loss :*

$$PL^R F^{U/H} = 30 * \log_{10}(D) + 18.9 * \log_{10}(f) + 36.85 + A \quad (10)$$

where  $A$  is the path attenuation due to rainfall which is given by Eq. (3).

The link margin due to heavy rainfall is given as

$$LM = \frac{G_t G_r P_t}{K T_s D_r (PL)_0 (PL)_{RF} (E_b/N_0)} \quad (11)$$

where  $G_t$  and  $G_r$  are transmitter and receiver antenna gains in dB respectively;  $P_t$  is the transmitter power in Watts;  $K$  is a Boltzman's constant;  $(PL)_0$  is the free space path loss in dB;  $T_s$  is the noise temperature;  $(PL)_{RF}$  is the path loss due to rainfall in dB;  $D_r$  is the data rate in bits/sec; and  $E_b/N_0$  is the ratio of energy per bit to noise spectral density.

## 4. OPTIMIZATION APPROACHES

In this paper, we consider GA and PSO algorithms as optimization approaches. These algorithms provide accurate optimization values for an objective function. Therefore, we consider these two algorithms to improve the performance of wireless networks by reducing the path loss and improving the link margin.

### 4.1. Genetic Algorithm

A natural selection procedure serves as the basis for the optimization method known as a genetic algorithm. It uses the "survival of the fittest" concept and is a population-based search method. The genetic operators are applied repeatedly to existing individual populations, and they create new populations to enhance the system's performance. The main components of GA are the representation of the chromosomes, selection, recombination, mutation, and evaluation of fitness functions, which are shown in the GA flowchart in Fig. 1. Simple GA has been transformed into multi-objective GA. Assigning fitness functions is where multi-objective GA (MOGA) and GA

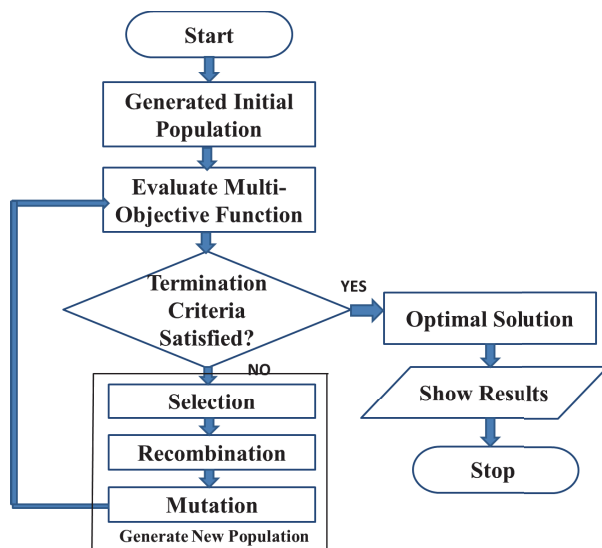


FIGURE 1. Genetic algorithm flowchart.

diverge. Multi-objective GA's main objective is to create the best Pareto front possible in the objective space, which ensures that no fitness function can be further enhanced without having an impact on the other fitness functions [56].

The step-by-step procedure of GA is summarized as follows:

- Initially, a counter is initiated to generate the initial population.
- By utilizing the individuals within the current population, the algorithm produces a sequence of new populations at each step.
- It calculates the fitness value for each individual within the current population and then converts the raw fitness scores into a range of usable values.
- Individuals with lower fitness values in the current population are transferred to the next population. These values give rise to optimal solution.
- The crossover and mutation genetic operators are applied to generate children from the parents. These children then replace the current population, forming the next generation.
- The procedure is repeated for many generations, and the best solution is identified as the individual with the smallest fitness value.
- Finally, the objective function is optimized by minimizing the fitness value of individuals within the population.

$$\text{pathloss objective function} = @PL(D, f) \quad (12)$$

$$\text{Fitness}_{\text{pathloss}} = \text{pathloss objective function}(D, f) \quad (13)$$

$$1 \text{ m} \leq D \leq 1000 \text{ m}$$

$$1 \text{ GHz} \leq f \leq 100 \text{ GHz}$$

Therefore, the genetic algorithm efficiently searches for and converges to a global minimum and maximum without the requirement of complex derivative computations. The optimization process utilized a GA package in MATLAB to achieve its goals. The parameters considered for optimization are the path difference and the operating frequency. Therefore, we considered path difference and operating frequency as decision variables in MOGA. The objective functions are determined as the minimization of PL and maximization of link margin. GA tuning is used to optimize the PL in both the scenarios and to achieve the desired PL by adjusting population size, mutation rate, and selection rate. We conducted a series of simulations to fine-tune the GA parameters with various combinations of population sizes, mutation rates, and selection rates. Based on the outcomes of these preliminary experiments, we observed that a population size of 12, a mutation rate of 2, and a selection rate of 1 yielded satisfactory results such as enhanced path loss and received power. The optimization process is carried out for a maximum of 50 iterations. In this paper, we compare the traditional MATLAB coding approach with the genetic algorithm approach for estimating PL and link margin in both the environments.

#### 4.2. Particle Swarm Optimization

The algorithm is a search-based method used to iteratively adjust the population of potential solutions to find the optimal solution of a given problem [37]. The flowchart of PSO algorithm is shown in Fig. 2.

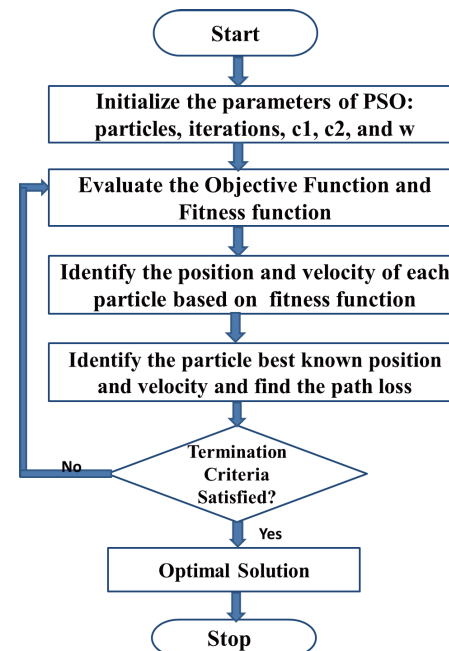


FIGURE 2. Particle swarm optimization algorithm flowchart.

The step-by-step procedure of PSO is summarized as follows [39]

- Initialization: Determine the maximum number of iterations and the number of particles in the swarm. Assign values to the social parameter ( $c2$ ) and cognitive param-

ter ( $c1$ ). Determine the inertia weight ( $w$ ) to balance exploration and exploitation.

- PL Model: Choose a suitable PL model and define the objective function based on the chosen path loss model.
- Initialization of particles: Initialize the position and velocity of each particle randomly within appropriate ranges based on the distance, frequency.
- Evaluate the path loss using the objective function for each particle's position. Set the particle's best-known position as its initial position and the particle's best-known path loss as the initial path loss value.
- Initialization of global best: Identify the particle with the best-known path loss among all particles. Set the global best-known position as the position of the best particle and the global best-known path loss as the path loss associated with the global best-known position.
- Main loop: Execute it for a specified number of iterations or until a convergence criterion is met.
- For each particle: Update the particle's velocity using cognitive and social influences and the inertia weight, using Eq. (5).

$$newVelocity = w * oldVelocity + c1 * rand() * (PersonalBestPosition - CurrentPosition) + c2 * rand() * (GlobalBestPosition - CurrentPosition) \quad (14)$$

Update the particle's position with the new velocity, using Eq. (6)

$$newPosition = currentPosition + newVelocity \quad (15)$$

Apply constraints to keep the particle's position within appropriate ranges.

- Evaluate the path loss at the new position using the objective function. If the new path loss is better than the particle's best-known path loss, then update the particle's best-known position and path loss.

After the PSO iterations, the global best-known position and path loss provides the optimized solution for minimizing the path loss in the given wireless communication scenario. In PSO optimization, we consider 100 iterations, 50 particles,  $c1 = c2 = 1.49445$ ,  $w = 0.729$ ,  $1\text{ m} \leq D \leq 1000\text{ m}$  and  $1\text{ GHz} \leq f \leq 100\text{ GHz}$  to estimate the best position, velocity, and path loss.

### 5. SIMULATION RESULTS

The impact of various weather conditions and various locations on mmwave signal propagation is estimated in this section. To determine the impact of frequent and intense rainfall on mmwave signal propagation, a number of PL models are explored [22]. We examine both LOS and NLOS propagation channels in the outside environment with rain attenuation. The operating frequency, path difference, and rainfall intensity are

all influenced by the path attenuation. The path attenuation resulting from rainfall is estimated in terms of path difference and operating frequency using Eq. (3). Using the ITU-R P.530-18 model, the path attenuation is estimated as 0.01% of the time of rain rate for various mmwave frequencies ranging from 10 GHz to 100 GHz with horizontal polarization [55, 57]. The horizontal polarization coefficient and constant  $K$  for mmwave frequencies from 1 GHz to 100 GHz are listed in Table 1 [55].

TABLE 1. Polarization coefficients.

Operating Frequency	Polarization Coefficient	$K$
10	1.2571	0.01217
20	1.0568	0.09164
30	0.9485	0.2403
40	0.8673	0.4431
50	0.8084	0.66
60	0.7656	0.8606
100	0.6815	1.3671

Figures 3 and 4 illustrate the path attenuation due to the path difference from 100 meters to 1 km and from 10 kms to 100 kms with various frequencies. These figures provide visual insights into how path attenuation varies with operating frequency and path difference. Notably, as both frequency and path difference increase, path attenuation also rises. Specifically, at lower frequencies, the impact of the path difference on path attenuation is minimal, whereas at higher frequencies, the effect is pronounced. This observation underscores the substantial impact of rainfall on higher frequencies of mmwave signals. Consequently, the extent of path attenuation is influenced by rainfall intensity, which in turn can significantly impact the overall performance of the communication system, particularly in mmwave based networks.

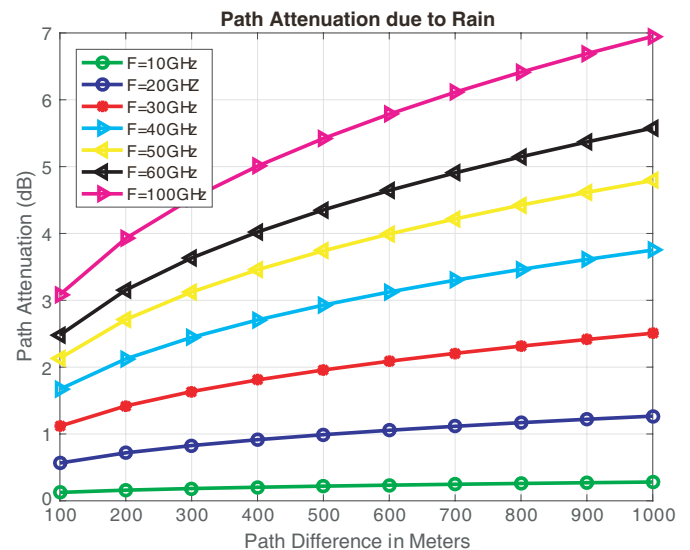


FIGURE 3. Path attenuation due to rain when path difference is in meters.

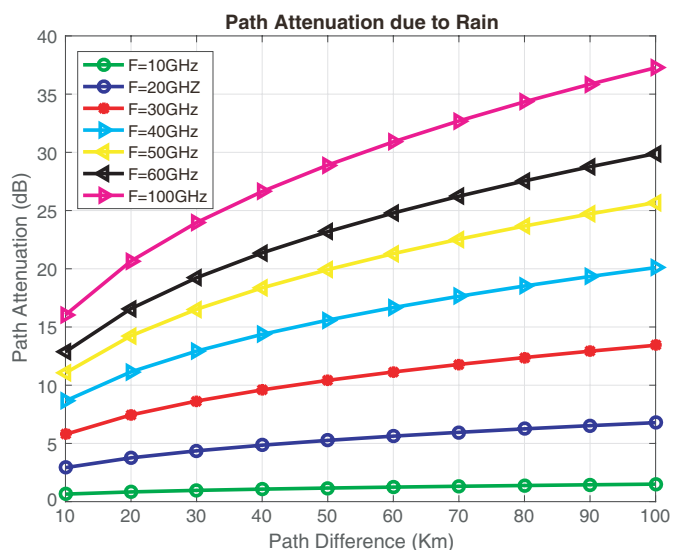


FIGURE 4. Path attenuation due to rain when path difference is in kilometers.

The investigation involves estimating PL within cities and highways for both LOS and NLOS paths. This estimation encompasses scenarios with and without rainfall, facilitated by Eqs. (7) through (12) and visualized in Figs. 5 to 10. The present study incorporates both theoretical and optimization-based methodologies to assess PL. Notably, the figures reveal the discernible impact of rainfall on PL, i.e., the PL is higher when there is rainfall than the PL without rainfall in cities and highway scenarios.

LOS path losses for cities and highways are shown in Figs. 5–8. These illustrations reveal a substantial increase in signal propagation within urban environments compared to highway settings. Friis’ law states that in a highway situation, propagating signals are weaker with distance. Since reflections from stationary barriers in street canyons are more likely to occur, the observed PL is significantly smaller, suggesting a wave-guiding effect.

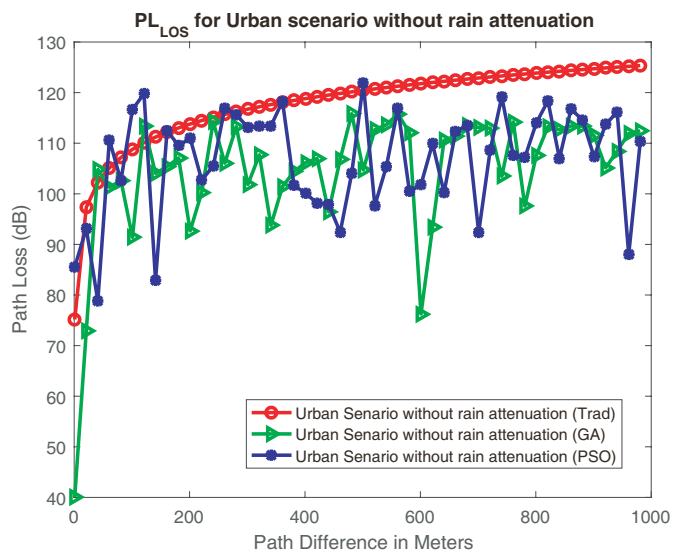


FIGURE 5. LOS Path loss of an urban scenario without rain attenuation.

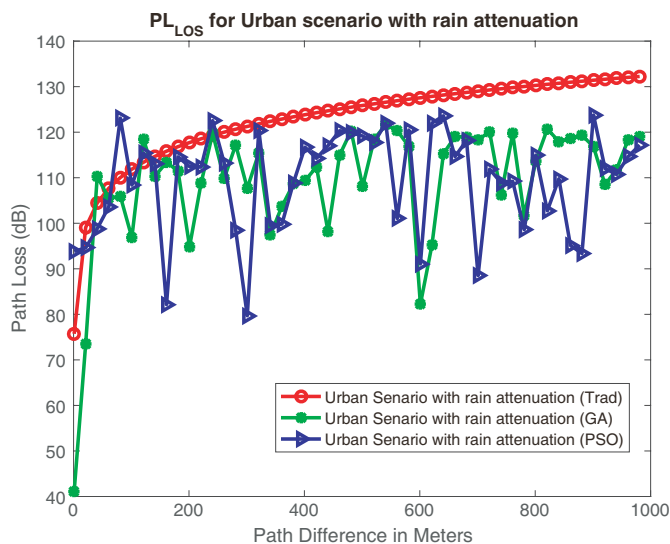


FIGURE 6. LOS Path loss of an urban scenario with rain attenuation.

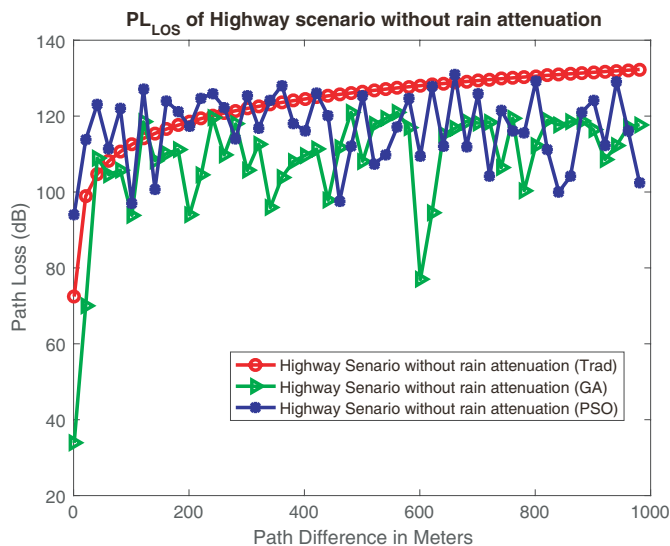


FIGURE 7. LOS Path loss of highway scenario without rain attenuation.

Figures 9 and 10 present the NLOS PL results for both urban and highway scenarios, considering the presence and absence of rainfall. As per the 3GPP models, there appears to be a consistent path loss across urban and highway settings [58]. The visual data underscores a significant increase in path loss during heavy rainfall, in contrast to clear sky conditions. Therefore, these findings collectively highlight the dependence of path loss on factors such as path difference, rainfall intensity, and operational frequency. Notably, PL and attenuation escalate alongside increased path differences, operating frequencies, and rainfall intensities. Moreover, the performance of path loss is intricately tied to variables like antenna height, tilt angle, and the positioning of the antenna [59, 60].

It is worth noting that the path loss derived through optimization methods is lower than the path loss resulting from conventional approaches. The optimization techniques exhibit a notable reduction in path loss compared to traditional methods within both urban and highway environments.

**TABLE 2.** Mean path loss in an urban and highway scenarios

Scenario	Environment	Mean Path Loss (dB)		
		Theo-retical	GA Approach	PSO Approach
LOS	Urban without Rain	117.64	104.52	106.29
	Urban with Rain	122.70	109.45	110.29
	Highway without Rain	123.10	108.29	116.86
	Highway with Rain	128.16	113.32	121.26
NLOS	Urban/Highway without Rain	150.63	133.85	141.99
	Urban/Highway with Rain	155.69	138.77	147.77

**TABLE 3.** Error statistics of an urban and highway scenarios.

Scenario	Environment	MSE (dB)		RMSE (dB)		SE (dB)		Accuracy (%)	
		GA	PSO	GA	PSO	GA	PSO	GA	PSO
LOS	Urban without Rain	4.99	3.21	2.33	1.79	1.84	1.44	88.85	90.35
	Urban with Rain	5.43	4.41	2.33	2.10	1.99	1.59	89.20	90.26
	Highway without Rain	6.46	3.91	2.54	1.98	2.14	1.34	87.97	94.93
	Highway with Rain	7.00	6.47	2.65	2.54	2.29	1.70	75.58	94.62
NLOS	Urban/Highway without Rain	9.80	8.72	3.10	2.95	2.88	1.87	88.86	94.26
	Urban/Highway with Rain	12.54	10.03	3.54	3.16	3.07	2.29	89.13	94.91

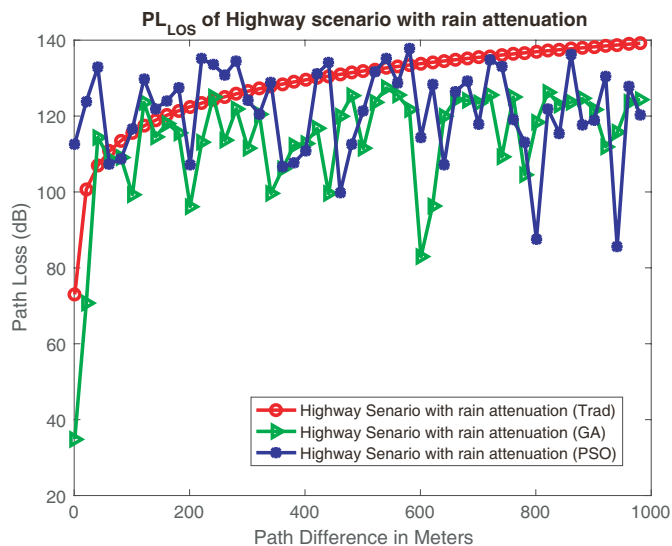


**FIGURE 8.** LOS Path loss of Highway scenario with rain attenuation.

The calculation of mean and error statistics, including metrics like mean square error (MSE), root MSE (RMSE), and standard deviation of error (SE), has been performed and compared across LoS and NLoS, as well as urban and highway scenarios. This analysis encompasses situations both with and without rainfall, whose results are displayed in Table 2 and Table 3. Across all scenarios, the employment of the PSO approach consistently yields diminished error statistics in contrast to the GA approach. Remarkably, the path loss optimization accomplished through PSO demonstrates heightened accuracy in comparison to GA optimization, boasting a remarkable 94% accuracy rate. This demonstrates that the optimization process significantly enhances system performance by minimizing path

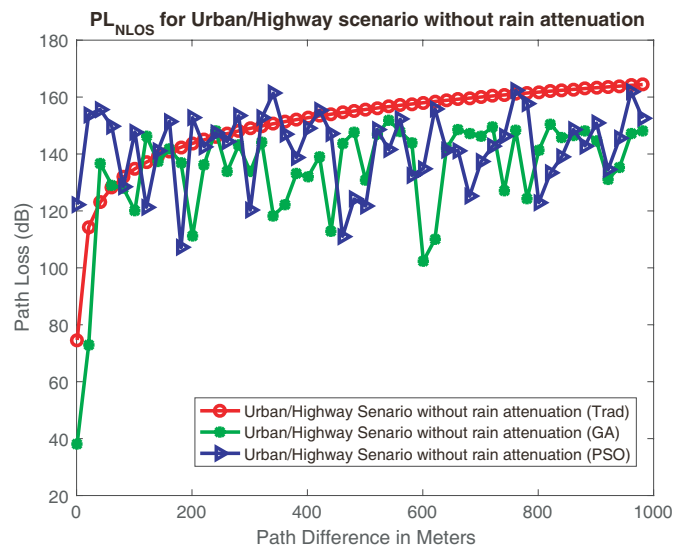


**FIGURE 9.** NLOS Path loss of an urban/highway scenario without rain attenuation.

loss in cities and highway environments, both with and without rainfall scenarios.

The link margin with rainfall attenuation is determined using Eq. (13). For mmwave frequencies ranging from 1 GHz to 100 GHz with path differences ranging from 100 m to 1 km, the connection margin is estimated as  $P_t = 27$  dBm,  $T_s = 30.62$  dB, and  $K = 1.38 \times 10^{-23}$  dB for varied antenna gains and free space PL. Illustrated in Fig. 11, the link margin experiences a marked reduction with the amplification of path differences. The examination of this graphical representation reveals that the link margin for the cities without rainfall surpasses that of the other five scenarios. Furthermore, a discernible disparity

TABLE 4. Optimal path difference.

Link Margin (dB)	Optimal Path difference (Meters)					
	$R^U$	$R_{RF}^U$	$R^H$	$R_{RF}^H$	$R1^{U/H}$	$R1_{RF}^{U/H}$
10	1325	870	868	615	225	180
15	1000	673	670	490	175	150
20	710	500	495	378	135	118

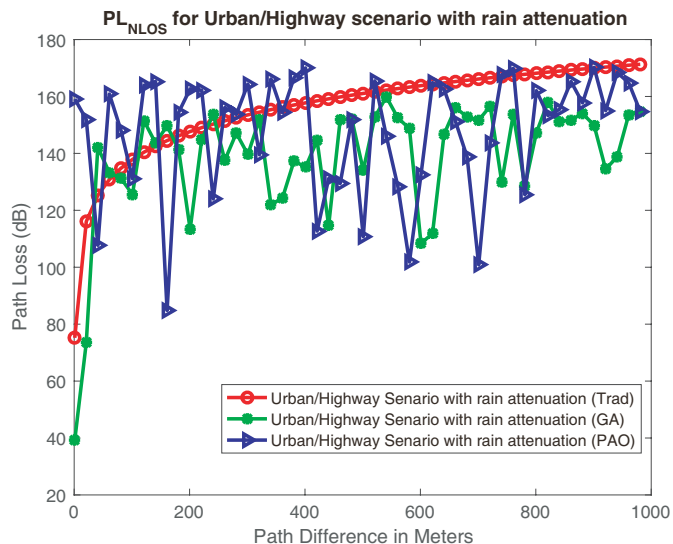


FIGURE 10. NLOS Path loss of an urban/highway scenario with rain attenuation.

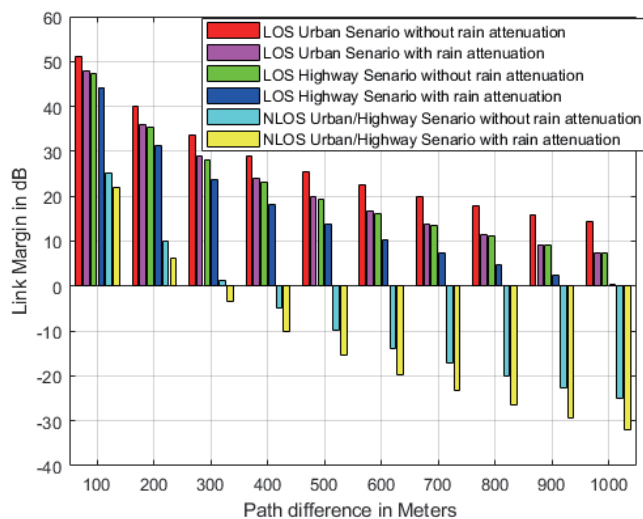


FIGURE 12. LOS and NLOS Link margin in urban and highway scenario with and without rain attenuation.

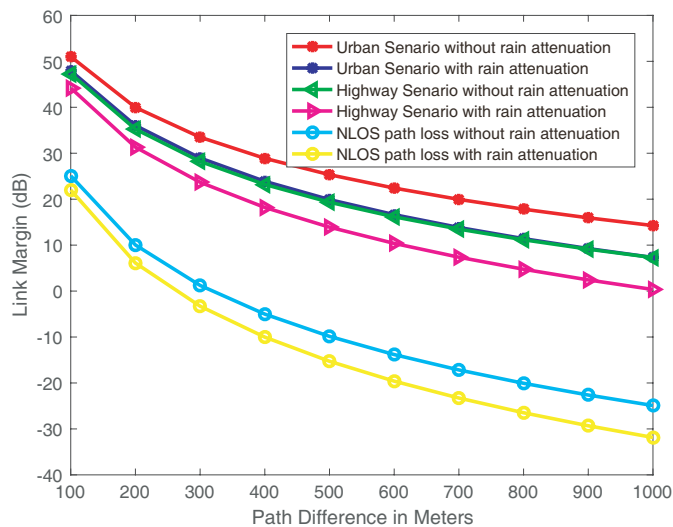


FIGURE 11. LOS and NLOS Link margin for the urban and highway scenario with and without rain attenuation.

is observed, where the LOS path exhibits a greater link margin than the NLOS path.

Illustrated in Fig. 12 is the dynamic change in link margin concerning the different path distances within both cities and highways. The examination of Fig. 12 yields estimations for the optimal path differences in both LOS and NLOS environments.

These estimations aim to achieve specified link margin thresholds of 10 dB, 15 dB, and 20 dB across diverse settings, encompassing urban and highway environments and accounting for varying rainfall conditions. The detailed findings of these estimations can be found in Table 4. Importantly, these optimized values are used to enhance throughput, data rates, and the system’s performance.

In Table 3,  $R^U$  and  $R_{RF}^U$  are the optimal path differences of urban scenarios without and with rain fall attenuation;  $R^H$  and  $R_{RF}^H$  are the optimal path differences of highway scenarios without and with rain fall attenuation;  $R1^{U/H}$  and  $R1_{RF}^{U/H}$  are the optimal path differences of urban or highway scenarios without and with rain fall attenuation. A review of Table 4 yields numerous important conclusions. First, it is noted that the urban scenario’s optimal path difference is greater than the highway scenario’s. The optimal path difference provides reduced path loss, and this reduced path loss improves the link margin and also data rates. From Eq. (11), it is observed that the path loss is inversely proportional to the link margin and data rates. To improve the received signal power, link margin, and data rates, we considered the optimal path difference in the case of heavy rainfalls in tropical regions. Therefore, the simulation results provide enhanced path loss and link margin for an optimal path difference. Reduced path loss and enhanced link margin are essential to enhancing throughput, coverage capacity, system performance, and data rates in wireless networks.



For applications involving connected automobiles, these optimal separations have significant implications, particularly in terms of mitigating the impact of rain. By optimizing the path difference, the impact of rain on connected car operations can be reduced, potentially reducing the traffic accidents during heavy rainfall. Overall, path difference optimization is a viable strategy for improving communication systems' reliability and efficiency during bad weather, which will promote safer and more effective transportation networks.

## 6. CONCLUSION

In this paper, we have investigated the impact of rainfall on mmwave frequencies of 5G communication networks for both urban and highway scenarios. Rainfall attenuation, LOS and NLOS probability, path loss, and link margin are estimated based on the outdoor probability models. The simulation results show that the path loss increases, and the link margin decreases as the path difference and rainfall rate increase. The impact of rainfall on path loss at higher frequencies is significantly higher than that at lower frequencies. The optimal path difference for urban and highway scenarios with and without rainfall is estimated and compared. The urban scenario without rainfall gives a higher optimal distance than the highway scenario with and without rainfall attenuation, and the urban scenario with rainfall attenuation achieves reduced path loss and enhanced link margin. Reduced path loss and enhanced link margin are essential to enhancing the throughput, coverage capacity, system performance, and higher data rates in wireless networks.

## ACKNOWLEDGMENT

This work is supported and funded by a Telekom Malaysia Research & development (TMR&D) grant, RDTG: 241126, MMUE/240081, Malaysia.

## REFERENCES

- [1] Faruk, N., A. Q. Ramon, S. I. Popoola, A. A. Oloyede, L. A. Olawoyin, N. Surajudeen-Bakinde, A. Abdulkarim, and Y. A. Adediran, "Spectrum survey and coexistence studies in the TV, WLAN, ISM and radar bands for wireless broadband services," in *2nd IEEE International Rural and Elderly Health Informatics Conference*, 2018.
- [2] Abuajwa, O., M. B. Roslee, and Z. B. Yusoff, "Simulated annealing for resource allocation in downlink NOMA systems in 5G networks," *Applied Sciences*, Vol. 11, No. 10, 4592, 2021.
- [3] Mohamed, K. S., M. Y. Alias, M. Roslee, and Y. M. Raji, "Towards green communication in 5G systems: Survey on beamforming concept," *IET Communications*, Vol. 15, No. 1, 142–154, 2021.
- [4] Nandi, D. and A. Maitra, "Study of rain attenuation effects for 5G Mm-wave cellular communication in tropical location," *IET Microwaves, Antennas & Propagation*, Vol. 12, No. 9, 1504–1507, 2018.
- [5] Zhang, L., H. Zhao, S. Hou, Z. Zhao, H. Xu, X. Wu, Q. Wu, and R. Zhang, "A survey on 5G millimeter wave communications for UAV-assisted wireless networks," *IEEE Access*, Vol. 7, 117 460–117 504, 2019.
- [6] Ullah, Y., M. B. Roslee, S. M. Mitani, S. A. Khan, and M. H. Jusoh, "A survey on handover and mobility management in 5G HetNets: Current state, challenges, and future directions," *Sensors*, Vol. 23, No. 11, 5081, 2023.
- [7] Rehman, A. U., M. B. Roslee, and T. J. Jiat, "A survey of handover management in mobile HetNets: Current challenges and future directions," *Applied Sciences*, Vol. 13, No. 5, 3367, 2023.
- [8] Crane, R. K., *Electromagnetic Wave Propagation Through Rain*, Wiley, 1996.
- [9] Lam, H. Y., L. Luini, J. Din, M. J. Alhilali, S. L. Jong, and F. Cuervo, "Impact of rain attenuation on 5G millimeter wave communication systems in equatorial Malaysia investigated through disdrometer data," in *2017 11th European Conference on Antennas and Propagation (EUCAP)*, 1793–1797, Paris, France, Mar. 2017.
- [10] Kourogiorgas, C., S. Sagkriotis, and A. D. Panagopoulos, "Coverage and outage capacity evaluation in 5G millimeter wave cellular systems: Impact of rain attenuation," in *2015 9th European Conference on Antennas and Propagation (EuCAP)*, 1–5, Lisbon, Portugal, Apr. 2015.
- [11] Zhang, Y.-P., P. Wang, and A. Goldsmith, "Rainfall effect on the performance of millimeter-wave MIMO systems," *IEEE Transactions on Wireless Communications*, Vol. 14, No. 9, 4857–4866, 2015.
- [12] Kestwal, M. C., S. Joshi, and L. S. Garia, "Prediction of rain attenuation and impact of rain in wave propagation at microwave frequency for tropical region (Uttarakhand, India)," *International Journal of Microwave Science and Technology*, Vol. 2014, No. 1, 958498, 2014.
- [13] Shrestha, S. and D.-Y. Choi, "Rain attenuation statistics over millimeter wave bands in South Korea," *Journal of Atmospheric and Solar-terrestrial Physics*, Vol. 152, 1–10, 2017.
- [14] Roslee, M., K. S. Subari, and I. S. Shahdan, "Design of bow tie antenna in CST studio suite below 2 GHz for ground penetrating radar applications," in *2011 IEEE International RF & Microwave Conference*, 430–433, Seremban, Malaysia, Dec. 2011.
- [15] Shayea, I., T. A. Rahman, M. H. Azmi, and M. R. Islam, "Real measurement study for rain rate and rain attenuation conducted over 26 GHz microwave 5G link system in Malaysia," *IEEE Access*, Vol. 6, 19 044–19 064, 2018.
- [16] Noh, S.-K. and D. Choi, "Propagation model in indoor and outdoor for the LTE communications," *International Journal of Antennas and Propagation*, Vol. 2019, No. 1, 3134613, 2019.
- [17] Naseem, Z., I. Nausheen, and Z. Mirza, "Propagation models for wireless communication system," *Signal*, Vol. 5, No. 01, 2018.
- [18] Sun, S., T. S. Rappaport, S. Rangan, T. A. Thomas, A. Ghosh, I. Z. Kovacs, I. Rodriguez, O. Koymen, A. Partyka, and J. Jarvelainen, "Propagation path loss models for 5G urban micro-and macro-cellular scenarios," in *2016 IEEE 83rd Vehicular Technology Conference (VTC Spring)*, 1–6, Nanjing, China, May 2016.
- [19] Zang, S., M. Ding, D. Smith, P. Tyler, T. Rakotoarivelo, and M. A. Kaafar, "The impact of adverse weather conditions on autonomous vehicles: How rain, snow, fog, and hail affect the performance of a self-driving car," *IEEE Vehicular Technology Magazine*, Vol. 14, No. 2, 103–111, 2019.
- [20] Sharif, S. M., "Attenuation properties of dusty media using Mie scattering solution," *Progress In Electromagnetics Research M*, Vol. 43, 9–18, 2015.
- [21] Musa, A. and B. S. Paul, "Prediction of electromagnetic wave attenuation in dust storms using Mie scattering," in *2017 IEEE AFRICON*, 603–608, Cape Town, South Africa, Sep. 2017.
- [22] Abuhdima, E. M. M., G. Comert, P. Pisu, C.-T. Huang, A. Elqouaq, C. Zhao, S. Alston, K. Ambrose, and J. Liu, "The

- effect of dust and sand on the 5G millimeter-Wave links,” in *2021 IEEE International Conference on Wireless for Space and Extreme Environments (WiSEE)*, 60–65, Cleveland, OH, USA, Oct. 2021.
- [23] Abuhdima, E., J. Liu, C. Zhao, A. Elqaouaq, G. Comert, C.-T. Huang, P. Pisu, and A. H. Nazeri, “Impact of dust and sand on 5G communications for connected vehicles applications,” *IEEE Journal of Radio Frequency Identification*, Vol. 6, 229–239, 2022.
- [24] Sudhamani, C., M. Roslee, J. J. Tiang, and A. U. Rehman, “A survey on 5G coverage improvement techniques: Issues and future challenges,” *Sensors*, Vol. 23, No. 4, 2356, 2023.
- [25] Tahir, M. N., P. Leviäkangas, and M. Katz, “Connected vehicles: V2V and V2I road pages=2356,d weather and traffic communication using cellular technologies,” *Sensors*, Vol. 22, No. 3, 1142, 2022.
- [26] Dutty, H. B. H. and M. M. Mowla, “Weather impact analysis of mmWave channel modeling for aviation backhaul networks in 5G communications,” in *2019 22nd International Conference on Computer and Information Technology (ICCIT)*, 1–6, Dhaka, Bangladesh, Dec. 2019.
- [27] Fencl, M., M. Dohnal, P. Valtr, M. Grabner, and V. Bareš, “Atmospheric observations with E-band microwave links—challenges and opportunities,” *Atmospheric Measurement Techniques*, Vol. 13, No. 12, 6559–6578, 2020.
- [28] Nymphas, E. F. and O. Ibe, “Attenuation of millimetre wave radio signal at worst hour rainfall rate in a tropical region: A case study, Nigeria,” *Scientific African*, Vol. 16, e01158, 2022.
- [29] Dimce, S., M. S. Amjad, and F. Dressler, “Mmwave on the road: Investigating the weather impact on 60 GHz V2X communication channels,” in *2021 16th Annual Conference on Wireless On-demand Network Systems and Services Conference (WONS)*, 1–8, Klosters, Switzerland, Mar. 2021.
- [30] Roslee, M. B., R. S. A. R. Abdullah, and H. Z. Shafr, “Road pavement density analysis using a new non-destructive ground penetrating radar system,” *Progress In Electromagnetics Research B*, Vol. 21, 399–417, 2010.
- [31] Govindarajulu, S. R. and E. A. Alwan, “Range optimization for DSRC and 5G millimeter-wave vehicle-to-vehicle communication link,” in *2019 International Workshop on Antenna Technology (iWAT)*, 228–230, Miami, FL, USA, Mar. 2019.
- [32] Alquhali, A. H., M. Roslee, M. Y. Alias, and K. S. Mohamed, “IoT based real-time vehicle tracking system,” in *2019 IEEE Conference on Sustainable Utilization and Development in Engineering and Technologies (CSUDET)*, 265–270, Miami, FL, USA, Nov. 2019.
- [33] Roslee, M., A. Alhammedi, M. Y. Alias, K. Anuar, and P. U. Nmenme, “Efficient handoff spectrum scheme using fuzzy decision making in cognitive radio system,” in *2017 3rd International Conference on Frontiers of Signal Processing (ICFSP)*, 72–75, Paris, France, Sep. 2017.
- [34] Kordi, K. A., A. Alhammedi, M. Roslee, M. Y. Alias, and Q. Abdullah, “A review on wireless emerging IoT indoor localization,” in *2020 IEEE 5th International Symposium on Telecommunication Technologies (ISTT)*, 82–87, Shah Alam, Malaysia, Nov. 2020.
- [35] Roy, S., J.-J. Tiang, M. B. Roslee, M. T. Ahmed, A. Z. Kouzani, and M. A. P. Mahmud, “Design of a highly efficient wideband multi-frequency ambient RF energy harvester,” *Sensors*, Vol. 22, No. 2, 424, 2022.
- [36] Roy, S., J. J. Tiang, M. B. Roslee, M. T. Ahmed, A. Z. Kouzani, and M. A. P. Mahmud, “Quad-band rectenna for ambient radio frequency (RF) energy harvesting,” *Sensors*, Vol. 21, No. 23, 7838, 2021.
- [37] Chen, Y. and N. Shang, “Comparison of GA, ACO algorithm, and PSO algorithm for path optimization on free-form surfaces using coordinate measuring machines,” *Engineering Research Express*, Vol. 3, No. 4, 045039, 2021.
- [38] Sooda, K. and T. R. Nair, “A comparative analysis for determining the optimal path using PSO and GA,” *ArXiv Preprint ArXiv:1407.5327*, 2014.
- [39] Garah, M., H. Oudira, L. Djouane, and N. Hamdiken, “Particle swarm optimization for the path loss reduction in suburban and rural area,” *International Journal of Electrical and Computer Engineering*, Vol. 7, No. 4, 2125, 2017.
- [40] Alfaresi, B., Z. Nawawi, and B. Y. Suprpto, “Development of path loss prediction model using feature selection-machine learning approach,” *International Journal of Advanced Computer Science and Applications*, Vol. 13, No. 10, 349–358, 2022.
- [41] Hashim, H. A., S. L. Mohammed, and S. K. Gharghan, “Path loss model-based PSO for accurate distance estimation in indoor environments,” *Journal of Communications*, Vol. 13, No. 12, 712–722, 2018.
- [42] Lian, B., Z. Wei, X. Sun, Z. Li, and J. Zhao, “A review on rainfall measurement based on commercial microwave links in wireless cellular networks,” *Sensors*, Vol. 22, No. 12, 4395, 2022.
- [43] Shayea, I., T. A. Rahman, M. H. Azmi, and A. Arsad, “Rain attenuation of millimetre wave above 10 GHz for terrestrial links in tropical regions,” *Transactions on Emerging Telecommunications Technologies*, Vol. 29, No. 8, e3450, 2018.
- [44] Han, C., J. Huo, Q. Gao, G. Su, and H. Wang, “Rainfall monitoring based on next-generation millimeter-wave backhaul technologies in a dense urban environment,” *Remote Sensing*, Vol. 12, No. 6, 1045, 2020.
- [45] Sen, P., J. Hall, M. Polese, V. Petrov, D. Bodet, F. Restuccia, T. Melodia, and J. M. Jornet, “Terahertz communications can work in rain and snow: Impact of adverse weather conditions on channels at 140 GHz,” in *Proceedings of the 6th ACM Workshop on Millimeter-Wave and Terahertz Networks and Sensing Systems*, 13–18, Oct. 2022.
- [46] Samad, M. A., F. D. Diba, and D.-Y. Choi, “A survey of rain attenuation prediction models for terrestrial links — Current research challenges and state-of-the-art,” *Sensors*, Vol. 21, No. 4, 1207, 2021.
- [47] Busari, H. O. and O. A. Fakolujo, “Rain attenuation prediction models in microwave and millimeter bands for satellite communication system: A review,” *FUOYE Journal of Engineering and Technology (FUOYEJET)*, Vol. 6, No. 1, 38–43, 2021.
- [48] Alozie, E., A. Abdulkarim, I. Abdullahi, A. D. Usman, N. Faruk, I.-F. Y. Olayinka, K. S. Adewole, A. A. Oloyede, H. Chiroma, O. A. Sowande, *et al.*, “A review on rain signal attenuation modeling, analysis and validation techniques: Advances, challenges and future direction,” *Sustainability*, Vol. 14, No. 18, 11744, 2022.
- [49] Samad, M. A., M. R. Ahmed, and S. Z. Rashid, “An overview of rain attenuation research in Bangladesh,” *Indonesian Journal of Electrical Engineering and Computer Science*, Vol. 23, No. 2, 902–909, 2021.
- [50] Imran, I. A. and S. M. Sani, “Prediction model for GSM signal attenuation in the abis interface during heavy rainfall in Nigeria,” *International Journal of Sciences: Basic and Applied Research (IJSBAR)*, Vol. 23, 147–155, 2015.
- [51] Singh, H., K. Saxena, V. Kumar, B. Bonev, and R. Prasad, “An empirical model for prediction of environmental attenuation of millimeter waves,” *Wireless Personal Communications*, Vol. 115, 809–826, 2020.

- [52] Alhilali, M., J. Din, M. Schönhuber, and H. Y. Lam, "Estimation of millimeter wave attenuation due to rain using 2D video disrometer data in Malaysia," *Indonesian Journal of Electrical Engineering and Computer Science*, Vol. 7, No. 1, 164–169, 2017.
- [53] Budalal, A. A. and M. R. Islam, "Path loss models for outdoor environment — with a focus on rain attenuation impact on short-range millimeter-wave links," *E-Prime — Advances in Electrical Engineering, Electronics and Energy*, Vol. 3, 100106, 2023.
- [54] Islam, R. M. D., Y. A. Abdulrahman, and T. A. Rahman, "An improved ITU-R rain attenuation prediction model over terrestrial microwave links in tropical region," *EURASIP Journal on Wireless Communications and Networking*, Vol. 2012, 1–9, 2012.
- [55] Series, I. R. P., "Specific attenuation model for rain for use in prediction methods," *Recommendation ITU-R*, 838–3, 2005.
- [56] Dash, S. and B. J. R. Sahu, "Genetic algorithm based coverage optimization 5G networks," *Journal of Information and Optimization Sciences*, Vol. 43, No. 5, 933–939, 2022.
- [57] P.530-18, R. I.-R., *Electronic Publication*, 2022.
- [58] Mondal, S. and D. Nandi, "Study of path loss models in V2V mm-wave communication," in *2022 URSI Regional Conference on Radio Science (USRI-RCRS)*, 1–3, Dec. 2022.
- [59] Yu, Y., Y. Liu, W.-J. Lu, and H.-B. Zhu, "Path loss model with antenna height dependency under indoor stair environment," *International Journal of Antennas and Propagation*, Vol. 2014, No. 1, 482615, 2014.
- [60] Roy, S., R. J.-J. Tiang, M. B. Roslee, M. T. Ahmed, and M. A. P. Mahmud, "Quad-band multiport rectenna for RF energy harvesting in ambient environment," *IEEE Access*, Vol. 9, 77 464–77 481, 2021.